Journal of Thermal Stresses
Publication details, including instructions for authors and subscription information:
http://www.tandfonline.com/loi/uths20

Final Shape of Precision Molded Optics: Part I—Computational Approach, Material Definitions and the Effect of Lens Shape

Balajee Ananthasayanam [a], Paul F. Joseph [a], Dhananjay Joshi [a], Scott Gaylord [b], Laeticia Petit [b], Vincent Y. Blouin [b], Kathleen C. Richardson [b], Daniel L. Cler [c], Matthew Stairiker [d] & Matthew Tardiff [d]

[a] Department of Mechanical Engineering, Clemson University, Clemson, South Carolina, USA

[b] School of Materials Science and Engineering, COMSET, Clemson University, Clemson, South Carolina, USA

[c] Benét Laboratories, Watervliet, New York, USAand Currently U.S. Army RDECOM/ARDEC, Picatinny Arsenal, New Jersey, USA

[d] Edmund Optics, Pennsburg, Pennsylvania, USA

Available online: 15 May 2012

To cite this article: Balajee Ananthasayanam, Paul F. Joseph, Dhananjay Joshi, Scott Gaylord, Laeticia Petit, Vincent Y. Blouin, Kathleen C. Richardson, Daniel L. Cler, Matthew Stairiker & Matthew Tardiff (2012): Final Shape of Precision Molded Optics: Part I—Computational Approach, Material Definitions and the Effect of Lens Shape, Journal of Thermal Stresses, 35:6, 550-578

To link to this article: http://dx.doi.org/10.1080/01495739.2012.674830

Journal of Thermal Stresses, 35: 550–578, 2012

ISSN: 0149-5739 print/1521-074X online
DOI: 10.1080/01495739.2012.674830

Taylor & Francis
Taylor & Francis Group

FINAL SHAPE OF PRECISION MOLDED OPTICS: PART I—COMPUTATIONAL APPROACH, MATERIAL DEFINITIONS AND THE EFFECT OF LENS SHAPE

Balajee Ananthasayanam[1], Paul F. Joseph[1], Dhananjay Joshi[1], Scott Gaylord[2], Laeticia Petit[2], Vincent Y. Blouin[2], Kathleen C. Richardson[2], Daniel L. Cler[3], Matthew Stairiker[4], and Matthew Tardiff[4]

[1]*Department of Mechanical Engineering, Clemson University, Clemson, South Carolina, USA*
[2]*School of Materials Science and Engineering, COMSET, Clemson University, Clemson, South Carolina, USA*
[3]*Benét Laboratories, Watervliet, New York, USA and Currently U.S. Army RDECOM/ARDEC, Picatinny Arsenal, New Jersey, USA*
[4]*Edmund Optics, Pennsburg, Pennsylvania, USA*

Coupled thermomechanical finite element models were developed in ABAQUS to simulate the precision glass lens molding process, including the stages of heating, soaking, pressing, cooling and release. The aim of the models was the prediction of the deviation of the final lens profile from that of the mold, which was accomplished to within one-half of a micron. The molding glass was modeled as viscoelastic in shear and volume using an n-term, prony series; temperature dependence of the material behavior was taken into account using the assumption of thermal rheological simplicity (TRS); structural relaxation as described by the Tool-Narayanaswamy-Moynihan (TNM)-model was used to account for temperature history dependent expansion and contraction, and the molds were modeled as elastic taking into account both mechanical and thermal strain. In Part I of this two-part series, the computational approach and material definitions are presented. Furthermore, in preparation for the sensitivity analysis presented in Part II, this study includes both a bi-convex lens and a steep meniscus lens, which reveals a fundamental difference in how the deviation evolves for these different lens geometries. This study, therefore, motivates the inclusion of both lens types in the validations and sensitivity analysis of Part II. It is shown that the deviation of the steep meniscus lens is more sensitive to the mechanical behavior of the glass, due to the strain response of the newly formed lens that occurs when the pressing force is removed.

Keywords: Aspherical glass lens; Deviation; Finite element method; Residual stresses; Structural relaxation; Temperature dependent properties; Viscoelasticity

Communicated by Martin Ostoja-Starzewski on 28 August 2011.

This material is based upon work supported in part by the U.S. Army Research Laboratory and the U. S. Army Research Office under contract/grant number ARO No. 56858-MS-DPS and by a DoD-ARO Cooperative Research Agreement, "Molding Science of IR Optics," through Benét Labs and Edmund Optics, with subcontract to Clemson University. The authors thank Dr. Ulrich Fotheringham of SCHOTT AG for his expert guidance concerning structural relaxation.

Address correspondence to Paul F. Joseph, Department of Mechanical Engineering, Clemson University, Clemson, SC 29634-0921, USA; E-mail: jpaul@clemson.edu

INTRODUCTION

Precision molded glass optics have recently gained in importance due to their cost-effectiveness for producing aspherical lens profiles [1–6]. Aspherical lens profiles are designed to precisely focus light at a single point and thus avoid optical aberration or blurring that occurs with conventional spherical lenses. Other advantages of using aspherical elements in optical devices include reduced lens count and thereby weight reduction, easier opto-mechanical assemblage and reduced internal reflection [3, 4].

The conventional lens manufacturing technique involves an iterative procedure of grinding, lapping and polishing to obtain a desired surface profile [4, 5]. Initially this technique was very costly, but continuous innovations in machining methods and efficient process planning have reduced the cost considerably. However, these innovations are limited to mass production of spherical lenses. The production of an aspherical lens surface requires specialized polishing techniques such as magneto-rheological finishing (MRF) and the precision polishing method [5]. Although these techniques can produce very high quality lens surfaces, the cost involved in production is very high and the byproducts, such as cutting fluids and lead from certain glass types, are dangerous to the environment. Additional references on these machining methods are given by Firestone et al. [4].

The precision lens molding process illustrated in Figure 1 is a cost effective alternative for low to medium volume production of aspherical lenses. The process begins with a glass preform, which has already undergone some machining, grinding and polishing prior to molding to define optic mass/volume and approximate spherical configuration. The preform is placed between dies and heated using, for example, infrared (IR) lamps, which are coiled around the dies. Once the glass becomes sufficiently softened, the lower die moves up and presses the lens to a desired center thickness. Then the entire assembly is cooled by a controlled flow of

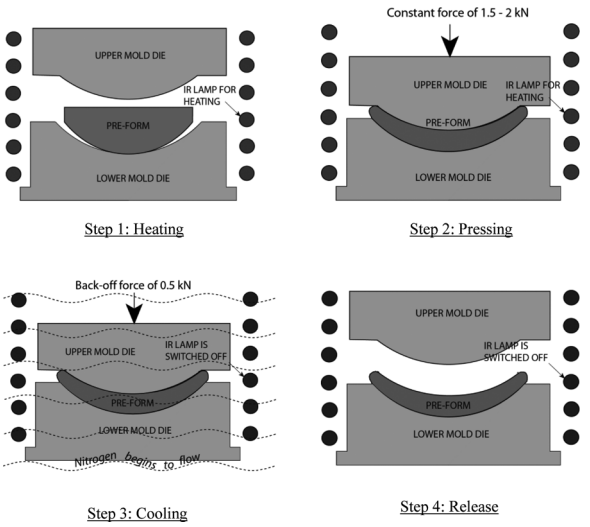

Figure 1 Illustration of the precision lens molding process.

nitrogen. The entire shaping process is done in one operation, which saves machine time and money.

Although the molding technique has advantages, several shortcomings must be overcome before applying the process to mass production. Some of the difficulties mentioned by Jain and Yi [3] include birefringence due to residual stresses created during molding, a short life of the expensive mold and/or mold coating due to glass/mold contact at high temperature, and adhesion of glass material to the mold surface [3]. From the point of view of the current study, the most important shortcoming is profile deviation, illustrated in Figure 2, which is caused by a shape change of the lens during cooling and is due to the complex thermo-mechanical behavior of glass and its strong temperature dependence. In order to control aberration, optical designers require a precise aspherical lens shape with specifications to less than one micron of profile deviation from the desired shape. The mold shape must therefore be "compensated" to achieve this desired shape, which corresponds to zero deviation. Throughout this study, however, the "desired shape" in Figure 2 is simply taken to be the mold shape at room temperature. Hence, the deviation corresponds to how much the lens deviates from the mold shape, which in practice can easily be 20 microns or more. Therefore, it is desirable to have an efficient method to determine the mold shapes to achieve a desired lens shape to within 1 micron deviation, or less.

A current approach of mold compensation is to empirically modify the size and shape of the molds by trial and error based on practical experience, to compensate for the temperature and time dependence of the material properties that give rise to the final molded part's shape. This approach results in large costs and extensive time required for the re-tooling of such high quality surfaces. This has motivated the development of computational approaches to create a compensated mold shape, which requires the prediction of the lens deviation within micron level accuracy, while taking into account the process parameters and the complex thermo-mechanical material behavior of glass.

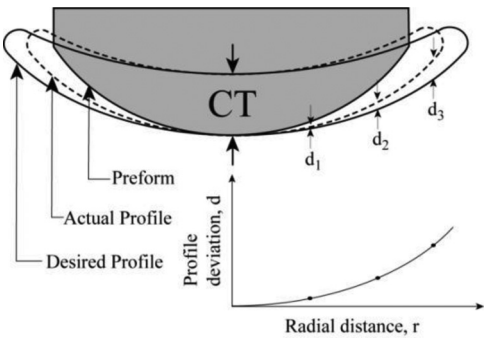

Figure 2 The schematic shows the preform, center thickness (CT) of the molded lens, desired lens profile, actual molded lens profile and the deviation, which is defined as the actual profile minus the desired profile. In the current study the desired profile is taken to be the mold profile at room temperature.

Literature

The precision lens molding process favors a relatively low pressing temperature where glass behaves as a viscoelastic material. Pressing at lower temperature protects the molds from chemical attack and minimizes shape change upon cooling. Therefore, the focus of this review will be on computational studies that address viscoelasticity [7], which is synonymous with stress relaxation. For studies at higher temperature, where glass can be modeled as a Newtonian viscous fluid, the reader can refer to the review paper by Brown [8] and some of the initial work of Yi and Jain [5, 9]. In the review that follows it is important to identify both the viscoelastic model used and how the parameters used in the material model were obtained.

Jain and Yi [10] modeled the pressing stage of lens molding for BK7 glass using displacement control. The cooling stage was not modeled in this study, which would involve the complex phenomenon of structural relaxation. Following an earlier paper [3], it appears that a no slip condition was used between the glass and the molds during pressing. The glass was assumed to be incompressible and the viscoelastic behavior for shear was obtained using relaxation data from a cylinder compression test. The elastic modulus was measured using a Brillouin light-scattering technique. Their experimental data show that the Young's modulus is fairly constant until the glass transition temperature range is reached when it drops drastically. Such behavior is also suggested qualitatively in Chapter 5 of Loch and Krause [11].

A comparison between maximum force measured and that obtained from the simulation is used for validation. Since the lens was not cooled, the prediction of deviation was not part of this study. In a later paper by Jain and Yi [9], the cooling stage was included and the effects of structural relaxation were taken into account using parameters from Scherer [12] for window glass. The viscoelastic response of the glass in shear was modeled using a single Maxwell element and as in the previous study, the glass was assumed to be incompressible. Complete sticking was assumed at the interface of the molds and glass. The Young's modulus of glass was assumed to be independent of temperature. Their main contributions are the identification of various material behaviors that can have significant effect on the outcome of the precision lens molding process and the experiments to obtain elastic and viscoelastic material behavior of a commercial molding glass in the molding temperature range.

Chang et al. [13] simulated a glass molding process where glass is modeled as a power-law strain-rate hardening material, which does not account for the time dependence of stresses and strain. A cylindrical compression test was performed on the glass at elevated isothermal temperature. Simulation was used to determine the parameters that define the hardening behavior and the friction coefficient by matching force-displacement and the shape of the barreling surface of the specimen. Prediction of deviation of the lens profile was not an objective.

Na et al. [14] simulated a molding process to predict the birefringence distribution in a molded lens. The main focus was not on the final geometry (deviation, center thickness) of the lens, but on the sensitivity of birefringence patterns for different preform shapes. The effects of structural relaxation were not included in the cooling stage of the process.

Sellier et al. [15] developed a finite element model of the lens molding process and coupled it with an optimizer to arrive at a compensated mold shape. This

research focused on optimization, i.e., arriving at the compensated mold shape by minimizing the mismatch between the actual and the desired mold geometry to within 1 μm. Although the predictions were not validated experimentally, computationally the method converges. The heat transfer model at the interface between the glass and the mold surfaces included radiation and conduction through air within the gap [16]. An advantage of the approach, according to the authors, is that it does not require the parameterization of the mold or the computation of the sensitivities with respect to different material and process parameters.

Arai et al. [17] developed finite element models for molding glass lenses using measured thermo-viscoelastic material properties for BK-7 and TaF-3, which are two widely used commercial optical glasses. Creep tests were conducted by compressing cylindrical glass specimens at multiple temperatures in the glass transition region. The viscoelastic material properties for shear and the shift factor were obtained from the measured data. Glass was assumed to be incompressible and friction was neglected. Structural relaxation behavior was approximated by assuming the thermal coefficient of expansion to be a fourth order polynomial function of temperature. The authors concluded that residual stresses in the molded lens are a strong function of the initial cooling rate.

A major obstacle to the use of computational analysis for glass molding is the lack of availability of material properties of glass that are relevant to the molding process. One goal of this study, which includes Parts I and II, is to use computational analysis to identify the key material properties that have an effect on deviation and substantiate the need to obtain them more accurately through experimentation.

THEORY

Glass Transition

The mechanical and thermal behaviors of glass are strongly temperature dependent. Referring to Figure 3 there are three distinct temperature regions: the glassy region, the transition temperature region and the liquid region. At high temperatures in the liquid region, glass behaves like a viscous fluid. At low temperatures in the glassy region, glass behaves like an elastic solid. Within the transition range, defined as $T_L < T < T_U$, which can extend for as much as 50–100°C around the glass transition temperature, T_g, the mechanical behavior is that of a viscoelastic fluid. The thermal expansion behavior of glass is instantaneous in the liquid and the glassy regions, although it is time-dependent in the transition region. This time-dependent behavior is referred to as *structural relaxation*, which also includes the time dependence of other properties such as specific heat, refractive index, density, viscosity and enthalpy. The glass transition temperature, T_g, is approximately the mid-point temperature of the transition region, but changes slightly during every heating and cooling cycle [12].

The temperature at which glass is molded is very crucial to the final shape and size of the lens [1]. Molding is not practical at temperatures below T_g, as high viscosity will require a large molding force that can result in damage to the tooling and the workpiece. If the glass is heated to a temperature much higher than T_g, molding becomes easier, but the contraction of the glass during cooling increases,

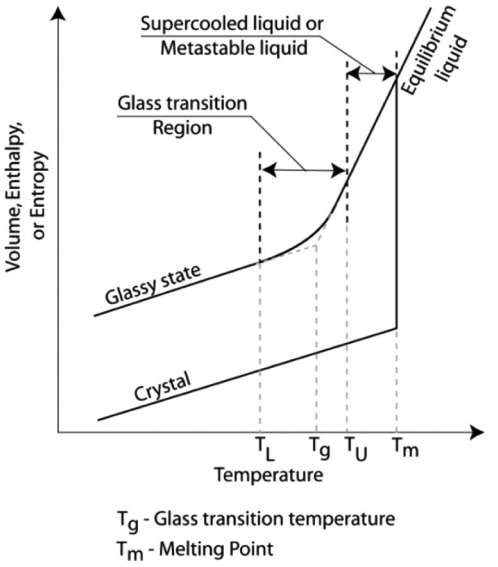

Figure 3 Comparison of volume change of glass to a crystalline material such as metal, during heating or cooling within the glass transition temperature region. The transition temperature region, $T_L < T < T_U$, defines temperatures where glass behaves visco-elastically [12].

which increases the deviation of the lens from the mold. Furthermore, adverse chemical reactions between glass and mold (i.e., glass volatilization and cross-contamination/constituent transfer) are more likely at high temperature, which can thus contribute to mold degradation. Because it is very difficult to control the cooling profile in time and space, and since mold degradation is a major obstacle for this technology, it is advantageous to press the lens at temperatures within the glass transition region, but above T_g. At these temperatures, glass behaves more as a viscoelastic material, although viscous flow is still the dominant mechanism that enables molding.

Viscoelasticity

Both shear and dilatational deformation behavior of glass exhibit viscoelasticity, i.e., a time-dependent strain response to a constant applied stress. The generalized Maxwell's model shown in Figure 4 is widely used to fit the viscoelastic response of glass. The constitutive equations of viscoelasticity [12] are given as follows:

$$s_{ij}(t) = \int_0^t G_1(t-t')\frac{\partial e_{ij}(t')}{\partial t'}dt' \tag{1}$$

$$\sigma(t) = \int_0^t G_2(t-t')\frac{\partial \varepsilon(t')}{\partial t'}dt' \tag{2}$$

where, respectively, s_{ij} and σ are the deviatoric and dilatational stresses, e_{ij} and ε are the corresponding deviatoric and dilatational strains, and $G_1(t)$ and $G_2(t)$ are the

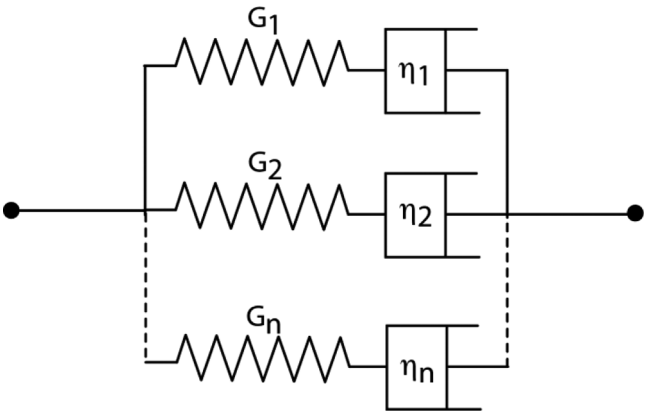

Figure 4 Generalized Maxwell's model for linear viscoelastic material behavior of glass.

deviatoric and dilatational (or volumetric) relaxation moduli. The relaxation moduli are expressed using the n-term prony series,

$$\psi_1(t) = \frac{G_1(t)}{2G_0} = \sum_{i=1}^{n_1} w_i e^{-t/\tau_i} \tag{3}$$

$$\psi_2(t) = \frac{G_2(t)}{3K_0} = \frac{K_\infty}{K_0} - \frac{K_\infty - K_0}{K_0} \sum_{j=1}^{n_2} v_j e^{-t/\lambda_j} \tag{4}$$

where G_0 is the instantaneous elastic shear modulus, K_0 is the instantaneous bulk modulus, K_∞ is the equilibrium bulk modulus, w_i and v_j are weighting factors for the deviatoric and volumetric relaxation functions and, τ_i and λ_j are the corresponding relaxation times for the deviatoric and volumetric relaxation functions, respectively. From (4) a non-zero equilibrium bulk modulus prevents any viscous flow or permanent deformation under volumetric loading, i.e., the material response due to hydrostatic loading is that of a viscoelastic solid. Thus, only the deviatoric strains contribute to permanent shape change.

Scherer [12] made use of the study by Li and Uhlmann [18] to argue that Newtonian viscosity behavior for the dashpots in Figure 4 is justified as long as the stresses developed in the material do not exceed 100 MPa. From a preliminary study of the molding process, the maximum stress was found to be less than 30 MPa during molding and hence, based on this argument, Newtonian behavior is used for the dashpots.

Thermo-Rheologically Simple (TRS) Behavior of Glass

Relaxation moduli are strongly temperature dependent as shown in Figure 5(a). Referring to Figure 5(b), the material is said to be thermo-rheologically simple (TRS) if on a log scale the relaxation moduli at different temperatures keep

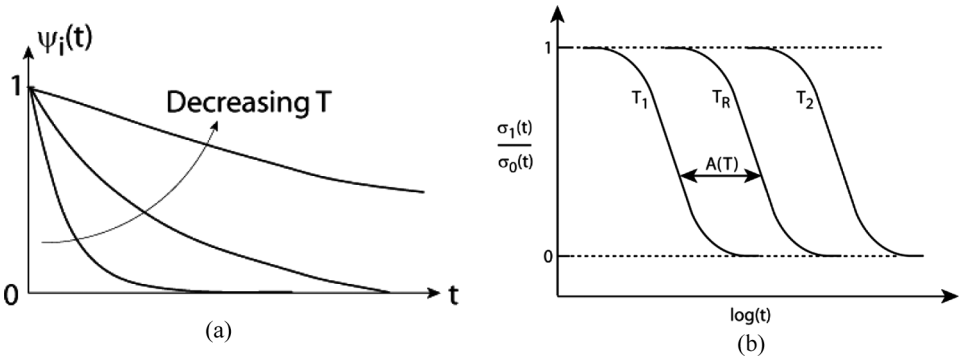

Figure 5 Thermo-rheologically simple (TRS) behavior of glass [12].

their shape but are shifted horizontally. Defining the shift factor as,

$$A(T) = \frac{\tau(T)}{\tau(T_R)}, \tag{5}$$

the temperature dependence can be approximated by the WLF (William–Landel–Ferry) equation as

$$\log A(T) = -\frac{C_1(T - T_R)}{C_2 + (T - T_R)}, \tag{6}$$

where T is the temperature at which the relaxation time is sought, T_R is the reference temperature and C_1 and C_2 are constants of the WLF equation [12].

Structural Relaxation

In the context of the current study, structural relaxation corresponds to temperature history dependent thermal expansion, which occurs within the glass transition temperature region. Therefore, within this temperature region, the value of the thermal expansion coefficient at each material point is a function of how the glass is cooled. To predict the final size and shape of a molded lens, it is necessary to calculate the thermal expansion in time and space for the entire lens during the molding process. In this section the physical behavior of volume change due to temperature change is discussed, followed by a presentation of the equations used to model it. This model, referred to as the Tool-Narayanaswamy–Moynihan (TNM) model, is based on an analogy with stress relaxation as discussed below [12, 19–21].

When glass is subjected to a *sudden change* in temperature within its transition temperature region, a time-dependent change in its volume occurs as shown in Figure 6. This time-dependent thermal expansion behavior is referred to as structural relaxation in the glass science literature. As discussed by Scherer [12], the term structural relaxation also applies to other properties. Referring to Figure 6, the liquid and glassy thermal expansion coefficients, denoted respectively by α_{VL} and α_{VG}, are constants for a particular glass type. In terms of these constants the

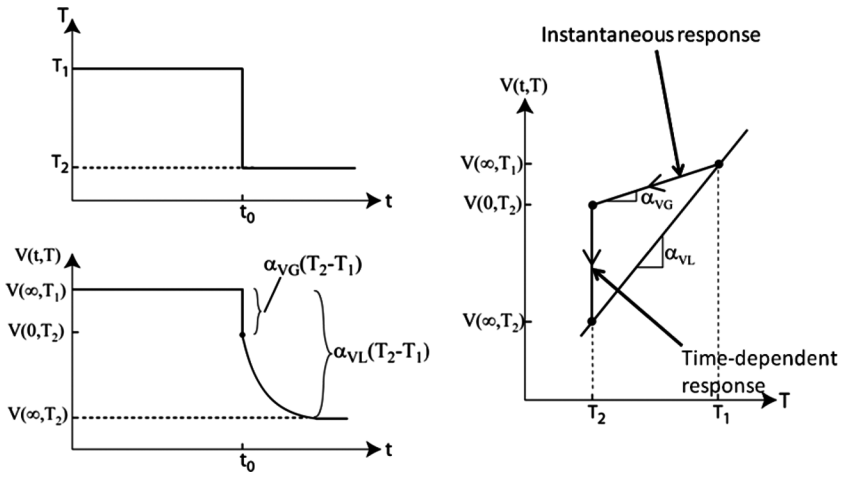

Figure 6 Effect of structural relaxation on volume of a glass specimen subjected to a sudden temperature change within the transition temperature range [12].

response in Figure 6 shows both an instantaneous and a time-dependent change in volume, which is analogous to stress relaxation and how strain responds due to a sudden change in stress. While the instantaneous change in volume occurs along the glass line with slope α_{VG}, the time-dependent change occurs in the vertical direction toward the equilibrium liquid line with slope α_{VL}.

Next consider the volume change of a glass sample that is *cooled continuously* at a constant rate as shown in the upper portion of Figure 7. The slope of the V-T curve, which is the thermal expansion coefficient, is presented in the lower portion of the figure. The behavior throughout the glass transition region is cooling rate-dependent, just as in stress relaxation the strain response is dependent on the rate at which stress changes. As the cooling rate decreases, the equilibrium value of the volume decreases. The analogy with stress relaxation is that the state of strain at a material point is a function of the entire stress history at that point. Concerning this analogy which was used by Tool [19] to develop the structural relaxation model, there is one important difference between stress and structural relaxation. In structural relaxation, material behavior is temperature dependent (as shown in the TRS model), while in stress relaxation, material behavior is assumed to be independent of the level of stress. Therefore, structural relaxation has a non-linear character compared to the linear theory of stress relaxation. For a formal understanding of the phenomena of structural relaxation and the details of the development of the TNM model used to address it, see the book by Scherer [12]. In the remainder of this section the characteristics of structural relaxation that are relevant to the simulation of the lens molding process are given.

When glass is in a liquid state, the volumetric thermal strain increment is defined as

$$d\varepsilon_V(t) = \alpha_{VL} dT \tag{7}$$

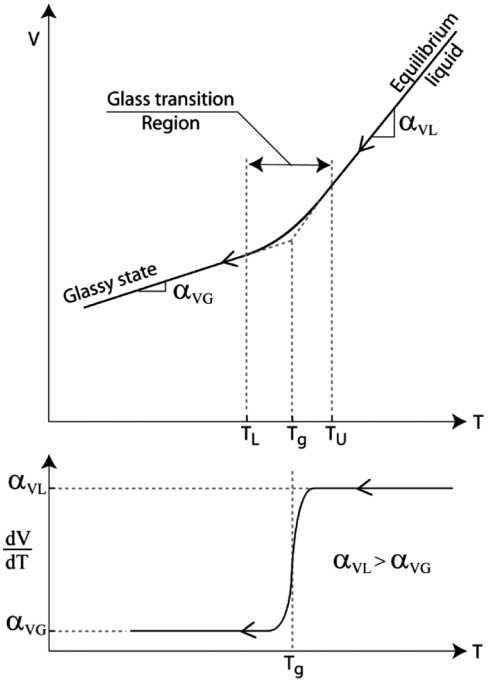

Figure 7 A typical Volume-Temperature curve of glass for a certain constant cooling rate is presented in the upper plot. The volume thermal expansion coefficient, α_V, i.e., the derivative of the volume with respect to temperature, is presented in the lower plot. Subscripts L and G refer to the expansion of the material in the liquid or glassy state, respectively.

and when it is in the solid, frozen or glassy state, the strain increment is defined as

$$d\varepsilon_V(t) = \alpha_{VG} dT. \tag{8}$$

However, when the glass is in the transition region between the solid and the liquid regions, the strain is not only dependent upon the temperature, but also on the fictive temperature, T_f, as defined below:

$$d\varepsilon_V(t) = \alpha_{VG} dT + (\alpha_{VL} - \alpha_{VG})\, dT_f. \tag{9}$$

The fictive temperature is purely a mathematical quantity that quantifies the state of the glass structure, and corresponds to the temperature at which the glass *would* be at equilibrium. The TNM-model of structural relaxation, which is based on the contributions of Tool [9], Narayanaswamy [20] and Moynihan [21], allows for the determination of the fictive temperature defined below,

$$T_f(t) = T(t) - \int_0^t M\left(\xi(t) - \xi(t')\right) \frac{dT_f}{dt'} dt', \tag{10}$$

where $M(\xi)$ is the structural relaxation function similar to stress relaxation function $G1(t)$ and $G2(t)$ in Equations (3–4). $M(\xi)$ can be represented as either a stretched

exponential,

$$M(\xi) = \exp\left[-\left(\frac{t}{\tau}\right)^{\beta}\right] \tag{11}$$

or by a prony series,

$$M(\xi) = \sum_{i=1}^{n} g_i \exp\left(-\frac{\xi}{\tau_i}\right) \ni \sum_{i=1}^{n} g_i = 1, \tag{12}$$

where 'β' is the Kohlrausch shape factor, 'τ' is the structural relaxation time, g_i are the weights of the prony exponenetials and τ_i are the prony relaxation times. In Equations (10–12), $\xi(t)$ is the reduced time defined by

$$\frac{d\xi(t)}{dt} = \exp\left[\frac{H}{T_R} - \frac{xH}{T(t)} - \frac{(1-x)H}{T_f(t)}\right], \tag{13}$$

where 'H' is the activation energy constant, T_R is the reference temperature at which the structural relaxation function, $M(\xi)$, is defined and x is the non-linearity parameter. If the structural relaxation function is defined as a prony series presented in Equation (12), then the fictive temperature can be written as a weighted summation of partial fictive temperature as follows:

$$T_f = \sum_{i=1}^{n} g_i T_{fi}. \tag{14}$$

Then Equation (10) can be re-written as the 'n' ordinary differential equations,

$$\frac{dT_{fi}}{dt} = -\frac{T_{fi} - T}{\tau_i}\frac{d\xi}{dt}, \quad i = 1, 2, \ldots, n. \tag{15}$$

Knowing the initial value of the fictive temperature and the four structural relaxation parameters H, x, β, and τ, Tool's equations (15) can be solved numerically for the partial fictive temperatures and the total fictive temperature can be calculated using (14). With the ability to determine the fictive temperature, the thermal strain increment can be determined using (9) and a history-dependent thermal expansion coefficient at the given temperature can be calculated. The implementation details of the structural relaxation phenomenon are presented later.

PRECISION MOLDING PROCESS

The Five Stages of Lens Molding

A Toshiba lens molding machine (GMP series) was used to mold a test lens made of OHARA L-BAL35 type glass and the process data from the machine is provided in Figure 8. This plot includes the temperature reading from a sensor placed on the outer periphery of the mold assembly, the applied molding force and the resulting displacement of the lower mold relative to the fixed upper mold as a function of time. All stages were carried out in a nitrogen environment. Although

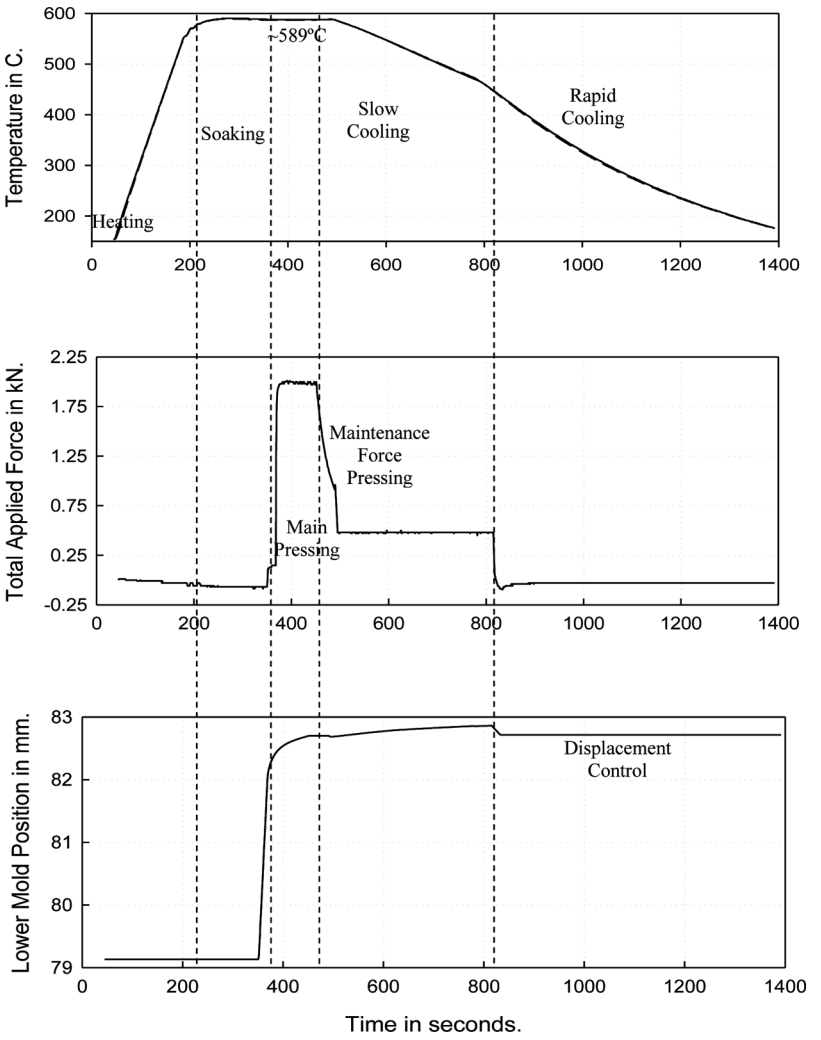

Figure 8 Process data from a Toshiba lens molding machine for a lens made of the molding glass, L-BAL35. This process data is used as the baseline for all results.

this process data was used for all results presented in Part I of this two-part series, for the sensitivity study in Part II, the data in Figure 8 define the baseline from which some of the process parameters are varied. The entire lens molding process takes approximately 23 minutes and the different stages used in both experiments and the simulations are:

(i) Heating (3.5 minutes),
(ii) Soaking (1.8 minutes),
(iii) Isothermal Pressing (2.17 minutes),
(iv) Slow cooling with maintenance force (5.3 minutes), and
(v) Rapid cooling stages (10.3 minutes).

Initial heating is carried out with infrared (IR) lamps that heat the molding assembly to the target molding temperature of 589°C. Once the sensor reaches this temperature, the preform is soaked at that temperature for 1.8 minutes. This soaking time is used prior to pressing because the temperature of the interior of the glass lags behind that of the sensor. It is our experience that a uniform temperature is not reached, which due to its importance is discussed in a separate section below. After soaking, the preform was pressed under a constant force of 2000 N at the molding temperature until a desired displacement is reached.

In this machine the force is controlled by a load cell attached to the lower mold. After this primary pressing stage, the slow cooling stage begins as the IR lamps are turned off and cold nitrogen begins to flow. During this slow cooling stage a "maintenance force" of 500 N is applied to prevent any gross shape changes as the glass is still hot and can deform easily. After this stage, the bottom mold is lowered creating a small gap, which reduces the force to zero. The displacement is fixed at this position for the remainder of the process. At the time the gap is created, a full flow of nitrogen is triggered which cools the entire assembly in approximately ten minutes. Due to the importance of the gap and its effect on heat transfer, thermal stresses and deviation, more details are given next.

Gap After Pressing

At the end of the slow cooling stage the maintenance force is removed by lowering the bottom mold by 0.15 mm to create a small gap. A small gap is essential to prevent cracking of the lens as it cools below the glass transition temperature. Furthermore, if the gap is too large, the heat transfer from the lens can be disproportionately high on one side making deviation difficult to control.

Because the gap is filled with nitrogen for the lens molding cases considered, the primary mode of heat transfer between the preform and the molds at this time is through contact/gap conductance, although radiation also contributes. Since gap conductance is inversely proportional to the thickness of the gap, knowledge of the position of the lens within the gap is crucial in predicting the temperature distribution in the lens, which in turn is crucial to predicting deviation of the molded lens. While in the current experiment, due to gravity the lens rests on the lower mold as a gap between the lens and upper mold is created, it is possible with some lens geometries for the lens to "stick" to the upper surface. The focus of Part I of this study is on how the creation of the gap affects the deviation for two different lens types. A sensitivity analysis of the profile deviation on the position of the gap is addressed in Part II, the second paper in this series.

Non-Uniform Temperature Distribution

Prior to pressing a soaking time of 2 minutes is used to heat the preform to a "molding temperature." Within this limited amount of time, the low thermal conductivity of glass makes it difficult for the temperature in the preform to be uniform and the high contact resistance at the mold/glass interface makes it difficult to reach the target temperature. Based on the analysis of the experimental displacement data from the molding machine and from experience in analyzing force-displacement data for a glass specimen used to characterize stress relaxation,

a non-uniform temperature below the target temperature is believed to exist. Since glass material behavior is strongly temperature dependent, this is a very important issue in the precise prediction of lens deviation, both from the experimental point of view for producing data to characterize material behavior and from the computational point of view if temperature cannot be predicted accurately.

Significance of Mold Coating

In the precision lens molding process, the mold surfaces that come into contact with the glass are usually coated due to the following reasons:

(i) chemically inert mold coatings prevent oxidation (though molding is often carried out in inert environments – N_2 or vacuum) and extend the life of the mold,
(ii) coated molds avoid sticking and chemical interaction/transfer of glass-mold constituents between the freshly molded lens to the mold surface,
(iii) low friction coatings increase mold life, reduce cycle time and therefore can reduce production cost.

In addition a low friction coating also affects the residual stress state in the lens and consequently, the final size and shape of the lens. In the current experiments the tungsten carbide molds had carbonized coatings.

MODELING DETAILS

The computational simulation of the lens molding process was done using the commercial finite element software, ABAQUS. Details associated with this implementation are described in the sub-sections below.

Finite Element Model of the Precision Molding Process

Using ABAQUS terminology, a *COUPLED-TEMPERATURE DISPLACEMENT type of analysis was used in the simulations due to the following couplings that exist between the mechanical and thermal boundary value problems:

(i) mechanical properties change drastically based on temperature, and
(ii) heat conduction at the glass/mold interfaces is affected by the changing surface of contact during pressing and the gap geometry at all stages of the process.

All five stages of the molding process discussed in Section III.1 were included in the simulation. The initial geometry of the model is shown in Figure 9. Since the preform and the molds are circular and the loading can be approximated as symmetric around the central axis, an axi-symmetric model was considered. The glass preform is modeled as a linear viscoelastic material, while both the upper and lower molds are modeled as linear elastic materials. The viscoelastic material properties of glass were extracted from the force-displacement data of glass specimens as described in the next section. The mold material properties and other glass properties, including structural relaxation, are tabulated next. The glass preform is meshed with 6900 CAX4RT elements, while the upper and lower molds

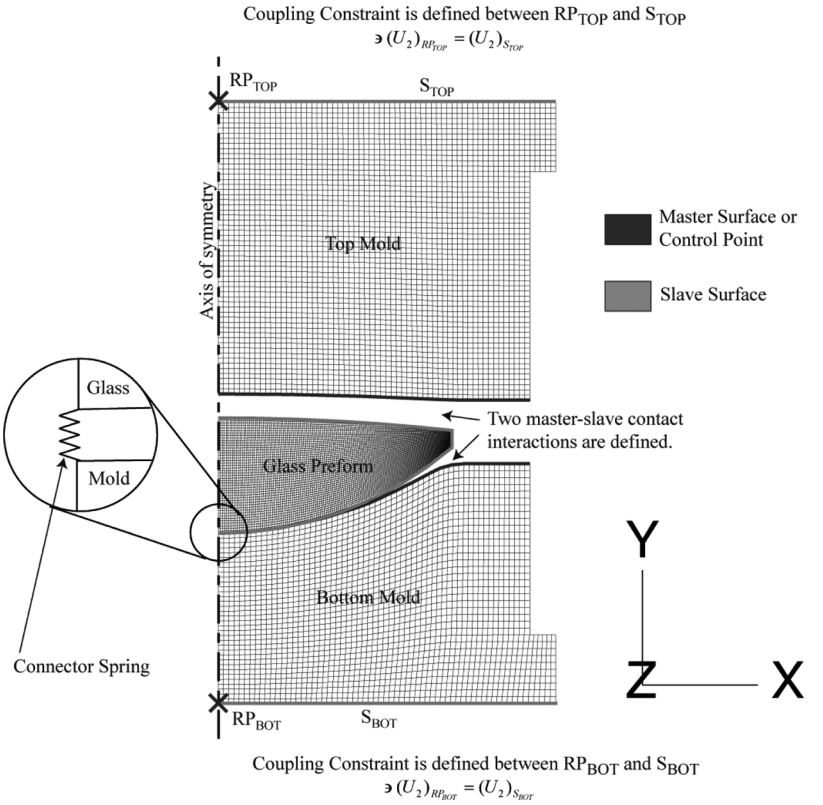

Figure 9 Illustration of the model geometry used in the simulations and all features that are valid throughout each simulation.

are meshed with 3485 and 2125 CAX4RT elements, respectively. Two master-slave types of contact interaction pairs were created as indicated in Figure 9. Normal contact was modeled using a "hard" contact formulation, while a Coulomb friction model based on a penalty formulation was used for the tangential behavior at the contact interface. In addition to radiation and conduction, heat transfer across the interface was accounted for using contact conductance.

Two coupling constraints are defined as indicated in Figure 9, where the vertical component of displacement of the slave surfaces was constrained to move with their respective master reference points, while the horizontal and rotational components of displacement are free. In addition to representing the actual process more closely, these coupling constraints make it easier to apply force boundary conditions and extract the displacement response.

Finally, as shown in Figure 9, an axial type of connector element (CONN2D2) is defined between the bottom most point that lies on the axis of the preform and the top most point that lies on the axis of the lower mold. As explained previously, a small gap is created at the end of the slow cooling stage. While in the actual process the lens usually attaches to the lower mold by gravity, which is not included in the model, a freshly molded lens with a concave upper surface sometimes attaches by

suction to the upper mold. This connector spring is only a mechanism to keep the freshly molded lens near a surface depending on experimental observation and does not alter the stress state in the lens. Therefore, a small value of 10 N/m was used for the stiffness of the connector spring.

Referring to Figure 9, in the first two stages of heating and soaking, both RP_{TOP} and RP_{BOT} are fixed. In the next stage contact between the molds and glass was established by moving RP_{BOT} by a specified distance, while RP_{TOP} is still fixed at the same position. Next a load was applied at RP_{BOT} defined by the process data in Figure 8, which fluctuates around 2000 N. In the next stage of slow cooling, the applied force was reduced to 500 N. As will be shown in the results, the simulations predict that this reduction in force causes most of the lens surfaces to lose contact with the molds. In the final rapid cooling stage, RP_{BOT} is moved down by a distance of 0.15 mm in about 19 seconds and held in this position. During this stage a relatively large gap is created between the glass and one of the mold surfaces. During both of these later stages, heat transfer from the glass to the molds takes place through contact/gap conductance, which is very sensitive to the size of the gap.

Temperature boundary conditions on the outer surfaces of the computational domain were applied as shown in Figure 10. A qualitative time history of the temperature shown is presented in this figure, which was assumed to be identical to the sensor temperature reading shown in Figure 8. In reality, the temperature is not

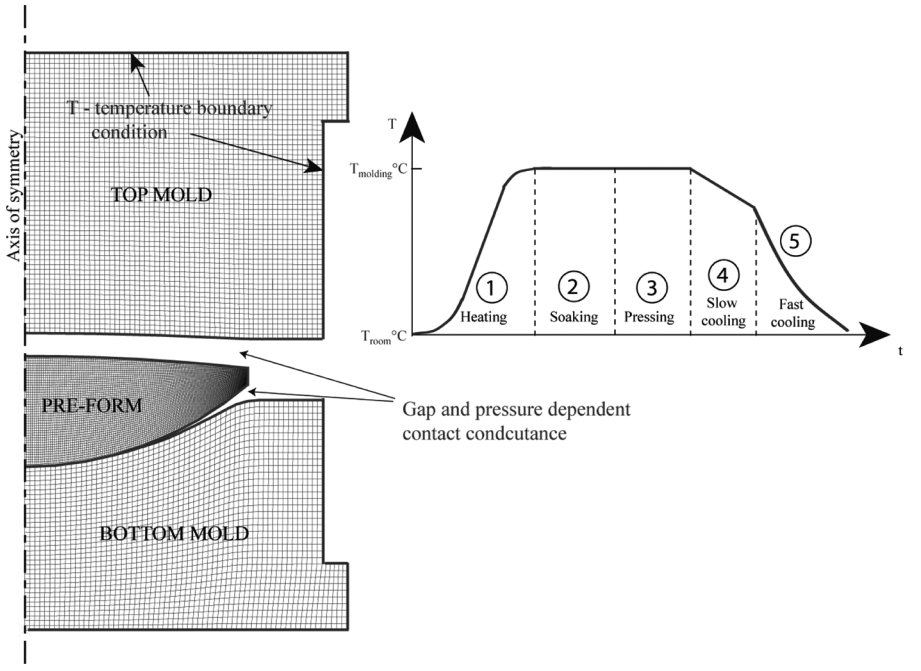

Figure 10 Illustration of the thermal boundary conditions applied in the five different stages of the molding process.

uniform at all the points on the outer surface of the mold. Any deviation from the sensor temperature value was neglected in the simulations.

Material Property Definitions

Several material property values used to define the baseline case are presented in this section. Just as with the process parameters, this baseline case is used without change in Part I, but is perturbed via sensitivity analysis in Part II.

The mechanical and thermal material properties of L-BAL35 molding glass and the Tungsten carbide (WC) molds are given in Table 1. The influence of the thin carbon coating has been assumed to be negligible in the calculations. The specific heat capacity, just as the thermal expansion behavior of glass described earlier, exhibits structural relaxation behavior. However, since sensitivity analysis showed that this is not a critical parameter for deviation, a simple step-wise function is used in this research that is consistent with the heating and cooling rates for the molding process.

The molding machine was used to generate creep curves for compressive loading using an annular disk of L-BAL35. These tests were done in a vacuum and at two different temperatures within the transition temperature range. These temperatures were initially believed to be 569 and 589°C, but were later determined to be closer to 551and 580°C, based on the temperature-viscosity data from Gaylord [22], which is believed to be a reasonable approximation of viscosity in this range of temperatures. These two temperature pairs form the basis of three different material sets that were used for results in both Part I and Part II of this two-paper series. The same level of force used in molding the lens from Figure 8 was used in these experiments, so the stress levels used to characterize the glass were approximately the same as those encountered in lens molding, which should help to minimize the effect of any nonlinear dependence on stress level if it exists. Annular disks were used since they were available from ring compression friction characterization as detailed by Ananthasayanam [26], which was also done in a vacuum.

The approach for the creep data was similar to that of Jain and Yi [10] and Arai et al. [17], except that these authors used solid disks and assumed that glass is incompressible. In the current study compressibility was taken into account so that a sensitivity analysis could be performed on the effect of the hydrostatic relaxation

Table 1 Thermal and mechanical properties of L-BAL35 glass and tungsten carbide

Property	Glass [22, 23]	Mold [24]
Density, ρ (kg/m^3)	2550	14650
Young's modulus, E (GPa)	See Table 2	570
Poisson's ratio	0.252	0.22
Specific heat, c_p (J/kg/K)	1100, $T \leq 470$°C	314
Thermal conductivity, κ (W/m/K)	1.126	38
Thermal expansion coefficient, α (K^{-1})	See Table 3	4.9×10^{-6}
Glass transition temperature, T_g (°C)	527	–

The viscoelastic and thermal expansion behaviors of the glass are presented in Tables 2 and 3, respectively.

function, G_2, function defined in (4). This function was approximated with a single term prony series. The associated weight factor of 0.85 was used determined based on a best fit of the data and taking into account the study by Dufferne et al. [25] for a type of Soda-Lime-Silica glass. Given this assumption, the shear function, G_1 defined in (3) was obtained from the creep data using ABAQUS with the measured friction coefficient.

The results of a prony series analysis are presented in Table 2 for three different material sets. Material Set 1 and Material Set 2, which essentially differ only in high temperature elastic modulus, should be considered as hypothetical glasses. Material Set 3 is believed to be the most representative of L-BAL35, as it has the most realistic TRS behavior and elastic modulus within the transition temperature range. In Material Set 1, a value of 0.8 GPa based on the creep curve data was used, whereas in both Material Sets 2 and 3, a more realistic value of 10% of the low temperature value (10 GPa) was assumed based on Loch and Krause [11]. The modulus varies linearly between the two constant values reported in Table 2. A more precise characterization of stress relaxation, such as that used by Dufferne et al. [25], which was only done at one temperature, was unfortunately beyond the scope of this study. However, it will be shown that the three data sets in Table 2 are sufficient for the current sensitivity and validation studies.

The thermal expansion behavior of glass is more complex than that of the molds and involves more parameters than a simple coefficient of thermal expansion, 'α' The structural relaxation experiments, the corresponding TNM model

Table 2 The three stress relaxation definitions of the molding glasses used in the current study

Shear relaxation function, $\psi_1(t) = \frac{G_1(t)}{2G_0}$		Hydrostatic relaxation function, $\psi_2(t) = \frac{G_2(t)}{3K_0}$		TRS behavior			Temperature dependent elastic modulus
w_i	τ_i (s)	$v_i = 1 - \frac{K_\infty}{K_0}$	λ_i (s)	T_R (°C)	C_1	C_2 (°C)	$E(T)$ (GPa)
Material set 1 (used in all simulations except Figure 3 of Part II)							
0.5794458	4.75	0.85	10	569	12.41	129	100.8, $T \leq 510$°C
0.3624554	6						
0.03	11						0.8, $T \geq 560$°C
0.028	930						
Material Set 2 (Figure 14 in Part I)							
0.5794458	0.38	0.85	10	569	12.41	129	100.8, $T \leq 510$°C
0.3624554	0.48						
0.03	0.88						10, $T \geq 560$°C
0.028	74.4						
Material Set 3 (Figure 14 in Part I and Figures 1 and 3 in Part II)							
1.0	2.504	0.85	10	550.8	7.96	110.8	100.8, $T \leq 510$°C 10, $T \geq 560$°C

Refer to Equations (3)–(6) for the functional forms. Material Set 3 approximates the behavior of the molding glass, L-BAL35, while Material Sets 1 and 2 should be considered as hypothetical glasses. At the reference temperature, T_R, the log of the equilibrium viscosity is 10.0 for all cases.

parameters introduced in Eqs. (10)–(13) and the implementation in the finite element software are described next.

The simulation accounts for both thermal and mechanical interaction between the glass preform and the mold. The molds are coated with a carbonized coating to prevent chemical reactions between glass and molds and also to facilitate the release of the lens at the end of the molding process. The tangential behavior is modeled using a penalty formulation and Coulomb friction. A ring compression test was used to characterize the friction at the interface and a base value of a friction coefficient of 0.04 was used. More details related to this test are given by Ananthasayanam [26]. The two surfaces can exchange heat by contact/gap conductance and radiation. The heat transfer between the surfaces that are either in contact or separated by a small gap is defined by

$$q = h_g(T_{\text{slave}} - T_{\text{master}}), \tag{16}$$

where 'q' is the heat flux per unit area in W/m^2, 'h_g' is the contact/gap heat transfer coefficient in $\text{W/m}^2/\text{K}$ and T_{slave} and T_{master} are the temperatures of the adjacent nodes of the contacting slave and master surfaces, respectively. The contact/gap heat transfer coefficient is defined by

$$h_g = \min\left(\frac{\kappa_{N_2}}{d}, 5000\right) \text{W/m}^2/\text{K}, \tag{17}$$

when surfaces are close but not contacting, and a pressure independent value of $h_g = 5000\,\text{W/m}^2/\text{K}$, when the smooth surfaces are in contact. The thermal conductivity of air, κ_{N_2} is $0.04\,\text{W/m/K}$ and 'd' is the gap distance between the two surfaces. The gap-dependent part of the contact conductance model is obtained from Madhusudana [16], while its maximum value is based on Sellier et al. [15]. This maximum limit for gap conductance is used to prevent the value from increasing to infinity as the surfaces come very close to each other. An infinite value means there is no resistance and the two surfaces are at the same temperature.

Heat transfer at the interface through radiation is given by

$$q = \frac{\sigma}{\left(\frac{1}{\varepsilon_{\text{slave}}} + \frac{1}{\varepsilon_{\text{master}}} - 1\right)} \left(T_{\text{slave}}^4 - T_{\text{master}}^4\right) \text{ W/m}^2 \tag{18}$$

where σ is the Stefan–Boltzmann constant ($5.67 \times 10^{-8}\,\text{W/m}^2/\text{K}^4$), $\varepsilon_{\text{slave}} = 0.85$ is the emissivity of the glass surface, and $\varepsilon_{\text{master}} = 0.15$ is the emissivity of the mold surface.

Structural Relaxation Implementation

Markovsky et al. [27] gave a semi-implicit finite difference scheme to solve Tool's Equations (15), which was used in the current study to determine the fictive temperature. Substituting Equation (13) in Equation (15), the differential form of Tool's equation is

$$\frac{dT_{fi}}{dt} = \frac{T - T_{fi}}{\tau_i} \exp\left[\frac{H}{T_R} - \frac{xH}{T(t')} - \frac{(1-x)H}{T_f(t')}\right], \quad i = 1, 2, \ldots, n, \tag{19}$$

with initial conditions $T_f(0) = T_0$ and $T_{fi}(0) = T_0$, when cooling from an initial temperature that is much higher than T_g. However, if heating was considered, say from room temperature, the initial conditions change to $T_f(0) = \sum_{i=1}^{n} v_i T_{fi}(0) = T_g$, where $T_{fi}(0)$ is a distribution around T_g whose value is dependent on the previous cooling rate. Using the backward-Euler method, Equation (19) is discretized to obtain

$$\frac{T_{fi}(N) - T_{fi}(N-1)}{dt} = \frac{T(N) - T_{fi}(N)}{\tau_i} \exp\left[\frac{H}{T_R} - \frac{xH}{T(N)} - \frac{(1-x)H}{T_f(N-1)}\right]. \tag{20}$$

Equation (20) is not a fully implicit discretization because the fictive temperature in the last term of the exponent is evaluated at t_{N-1} and not at t_N. This makes the solution of the differential equation for $T_{fi}(N)$ easier to obtain than in the fully implicit case and without loss of accuracy. Markovsky et al. [27] proved that this method is unconditionally stable for any time step, Δt, smaller or larger than any of the relaxation times.

The structural relaxation behavior of glass can be implemented in ABAQUS using the UEXPAN subroutine by adding time-dependence to the thermal expansion coefficient. The user subroutine was written in Intel Visual Fortran that is compatible with ABAQUS.

The input parameters required for modeling structural relaxation behavior in the finite element code were obtained from experiments conducted on a Thermo-Mechanical Analyzer (TMA) and Differential Scanning Calorimetry (DSC). More details on the experimental techniques, their drawbacks and methods of extraction of parameters are discussed in Gaylord et al. [28]. The TNM-model parameters based on DSC measurements have to be converted to a form that is acceptable by the finite element code. The TNM-model parameters of structural relaxation based on differential scanning calorimetry (DSC) are $(\Delta H/R, x, \beta, \tau_0)$. However, the finite element implementation selected in the current study, which was adopted from the sandwich seal solution given by Scherer and Rekhson [29], requires the structural relaxation parameters $(\Delta H/R, x, \beta, \tau_R)$ defined at a reference temperature T_R. The structural relaxation time at any temperature based on the TNM-model is defined by

$$\tau(T) = \tau_0 \exp\left[\frac{\Delta H}{R}\left(\frac{x}{T} + \frac{1-x}{T_f}\right)\right]. \tag{21}$$

To convert the DSC structural relaxation parameters to a form suitable for the finite element code, an arbitrary temperature, T_R that is 50°C to 100°C higher than the glass transition temperature, T_g is used as a reference temperature. Since the structural relaxation process is faster at higher temperature, the difference between the actual and the fictive temperature will be negligible and allows for the following relationship:

$$\tau_R = \tau(T_R) = \tau_0 \exp\left[\frac{\Delta H}{R}\left(\frac{1}{T_R}\right)\right]. \tag{22}$$

Table 3 Material parameters for TNM model of structural relaxation of L-BAL35 glass

Solid coefficient of thermal expansion, $\alpha_g(K^{-1})$	OHARA specification sheet	8.1×10^{-6}
	Gaylord et al. [28]	$(8.2 \pm 0.1) \times 10^{-6}$
Liquid coefficient of thermal expansion, $\alpha_l(K^{-1})$		$(70 \pm 0.1) \times 10^{-6}$
Activation energy constant, $\frac{\Delta H}{R}K$	Gaylord et al. [28]	$90,608 \pm 4531$
Nonlinearity parameter, x		0.745 ± 0.04

Relaxation function			
Kohlrausch stretched exponential		Prony series ($T_R = 589°C$)	
β	τ_0 (s)	w_i	τ_i (s)
0.802 ± 0.04	$(2.44 \pm 0.13) \times 10^{-47}$	0.003004	0.00016565
		0.0117675	0.00161635
		0.04106065	0.0086500
		0.1431509	0.0342118
		0.4401423	0.1000290
		0.3608743	0.1984004

Now that the stretched exponential function that describes the structural relaxation phenomenon at the reference temperature is known, a nonlinear curve fitting routine in MATLAB was used to convert it into a prony series defined here:

$$\exp\left[-\left(\frac{t}{\tau_R}\right)^{\beta}\right] = \sum_{i=1}^{n} v_i \exp\left(-\frac{t}{\tau_{Ri}}\right), \quad \sum_{i=1}^{n} v_i = 1. \tag{23}$$

Specifically, a 6-term prony series was used to approximate the stretched exponential relaxation function. The structural relaxation parameters along with the liquid and solid thermal expansion coefficients used in this research are provided in Table 3, which were obtained from Gaylord [22].

RESULTS

In this two-part series three different lens geometries were used; one bi-convex lens that is often referred to as the "validation" case and two steep meniscus lenses that are very similar. Only the bi-convex lens and one of the steep meniscus lenses are used for results in Part I. The second steep meniscus lens is used in a combined validation and sensitivity study in Part II.

Convergence Study for a Bi-Convex Lens

The profile deviation, or simply deviation, is defined herein as the difference between the final lens shape and that of the mold at room temperature, i.e., the "desired profile" in Figure 2 is the mold shape. All results correspond to a material defined by the properties in Tables 1–3, which were obtained from experimental data and from the literature. Although this glass is intended to be LBAL-35, if one or more of the material characterizations of the various input parameters are not accurate, then it is possible to generate results that do not agree with the actual

molding of this glass type. In this regard, gap conductance and stress relaxation, including initial elastic modulus and viscosity, are of the most concern.

The initial and final geometries of the bi-convex lens used for convergence in Part I are shown in Figure 11. To show that the model has converged and produced a mesh independent solution, three solutions using different meshes are presented in Figure 12. For these results Material Set 1 from Table 2 was used for stress relaxation. In addition to increasing the mesh from 4544 to 6959 elements for the preform in the very fine mesh, the strain-error tolerance has also been reduced from 0.005 to 0.001. Strain-error tolerance or CETOL parameter as defined in ABAQUS is the maximum difference between two consecutive creep strain increments, which controls the accuracy of the integration scheme. The run time on a DELL dual quad core 64-bit processor with 16 GB of memory is 45 minutes for the fine mesh and 70 minutes for the very fine mesh. In subsequent studies the fine mesh will be used.

The Effect of the Gap on the Evolution of Deviation

As the results in this two-part series will show, the deviation is a combination of thermal contraction due to cooling, stress relaxation behavior during the slow cooling stage, and the stress state in the lens when the maintenance force is removed. The primary mechanism of shape change for a well-chosen set of process parameters is thermal contraction, and this will be shown in Part II by performing a sensitivity analysis with the associated parameters. The effect of stress relaxation behavior, however, is more difficult to quantify and depends on the time dependent stress state

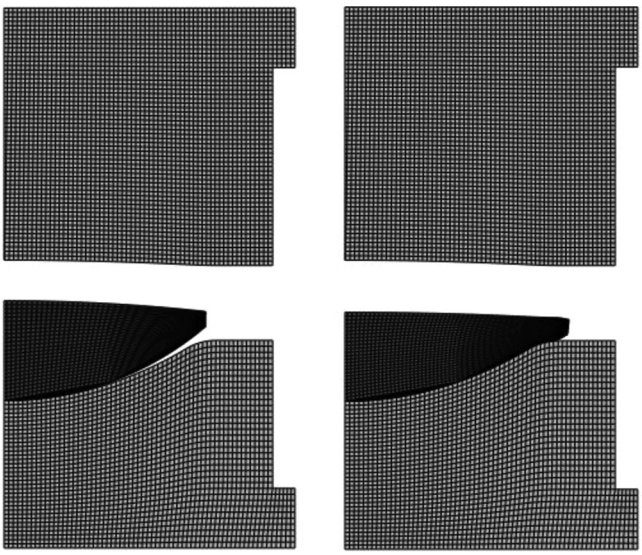

Figure 11 Computational models of the initial and final deformed configurations for the bi-convex lens. The preform on the left has two spherical surfaces, while the final pressed lens on the right has an aspherical lower surface.

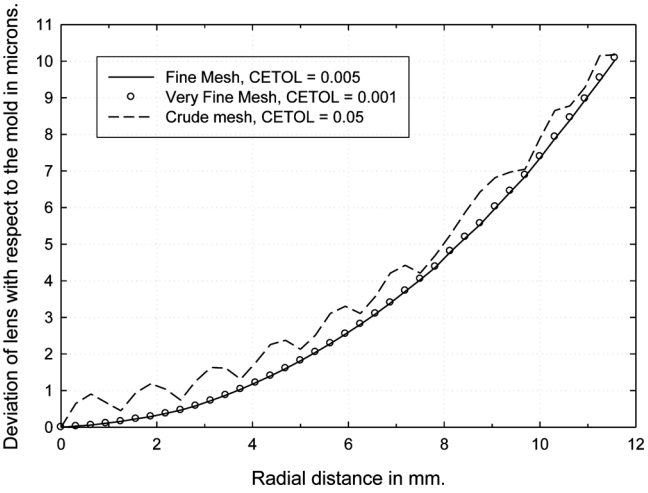

Figure 12 Convergence study of the deviation based on three different meshes and strain-error tolerances values (CETOL). The maximum error between the fine and very fine meshes is less than 0.05 microns.

in the lens. The stresses in the glass, which are generated during pressing and decay during the slow cooling period under the influence of the maintenance force, are highly dependent on the lens shape and the temperature dependent stress relaxation behavior of the glass. Because lens shape plays a key role in the stress state, the steep meniscus lens geometry shown in Figure 13 is introduced as a contrast to the bi-convex geometry in the studies that follow. A comparison of the final deviation for the steep meniscus lens to that of the bi-convex lens geometry is presented in Figure 14.

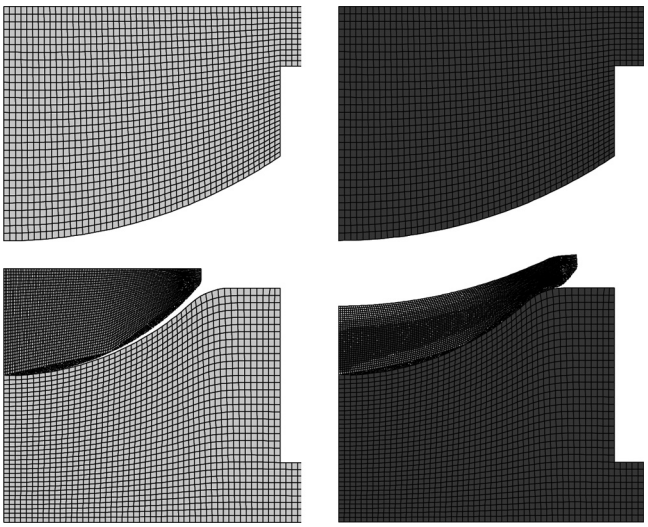

Figure 13 Initial and final deformed configurations for the steep meniscus lens.

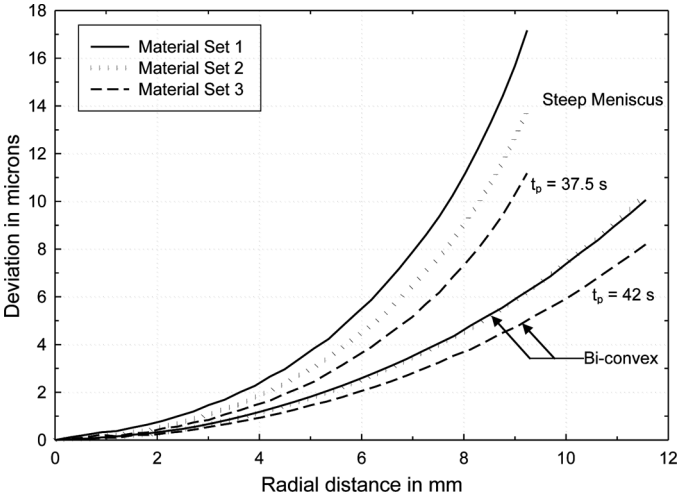

Figure 14 Deviation of the steep meniscus and bi-convex lenses for the three different stress relaxation behaviors listed in Table 2. For Material Sets 1 and 2 the press time, $t_p = 127$ s, which agrees with the press time in Figure 8. Press time was lowered for the Material Set 3 results as indicated, in order to maintain a constant value of center thickness.

The smaller radius of curvature in the steep meniscus case produces a larger deviation, since a flat surface will have the least deviation. For these results the three material behaviors from Table 2 are used for both lens types. For Material Set 3 it was necessary to lower the press time to maintain a constant value of the lens center thickness. The effect of the elastic modulus at high temperature is isolated by comparing the results for Material Sets 1 and 2. It is observed that by changing the elastic modulus, the deviation is affected only in the steep meniscus lens. The effect of a change in TRS behavior is observed by comparing the results of Material Sets 2 and 3. In this case the deviation for both lens types is affected, which is consistent with a lower press time due to the lower viscosity. A shorter press time for the Material Set 3 results corresponds to less heating and therefore lower peak temperature.

Cooling from a lower temperature experiences less thermal contraction, which reduces the deviation as shown in Figure 14. However, in addition to this temperature effect, there is also a superimposed stress effect due to the different TRS behaviors. The effect of stresses will be isolated in Part II of this study by performing a numerical experiment in which the temperature effect is minimized for different TRS behaviors (see Figures 9 and 10 in Part II and the related discussion). The focus in the current study, however, is on understanding the significant effect of the lens geometry due to changing only the elastic modulus.

To isolate the effect of stresses generated during molding from thermal effects, a simple numerical experiment was performed in which all thermal strain was "turned off" in the computational model for both the molds and the glass. Therefore, the only factors causing the deviation are mechanical, although the mechanical properties are still temperature dependent. This numerical experiment isolates the effect of stresses generated in the glass due to pressing and friction.

The deviations for the two lens types are presented in Figure 15 for Material Set 1, which show clearly that the steep meniscus has a non-negligible positive deviation, while the validation case is nearly zero. The results of Figures 14 and 15 show that for certain geometries the effect of the stress state in the lens has an influence on deviation.

The critical difference between the two lens geometries takes place when the gap is created at the end of the slow cooling stage. Referring to the process parameters in Figure 8, this gap of 0.15 mm is created by lowering the lower mold at a constant rate for 19 s. In Figure 16 the history of the deviation is plotted for Material Set 1, which shows that a significant shape change of five microns occurs for the steep meniscus lens, within one second after the gap starts to open, while nothing dramatic occurs for the bi-convex lens at this time. For the case of Material Set 3 this 5-micron change reduces to about one micron. To understand the difference between the two lens types, an examination of how the lens is supported by the molds during the slow cooling stage is required. As indicated in the schematic of Figure 17 and following Figure 8 for the sequence of events, after the pressing force drops from 2000 N to 500 N, most of the lens looses contact with the molds. The key difference between the two lens types is the "F_3" force applied to the center of the steep meniscus lens. When the 500 N force is removed by lowering the lower mold to create the 0.15 mm gap, the meniscus lens "springs" into a new shape, which is the explanation for the sudden change indicated in Figure 16. Most of the deviation change for the steep meniscus lens occurs within the first second of this 19 second period, which suggests an elastic response consistent with the results of Figure 14. The effect of the removal of this force is quantified in Figure 18 by plotting the radial stress at the sections indicated in Figure 17. It is observed that

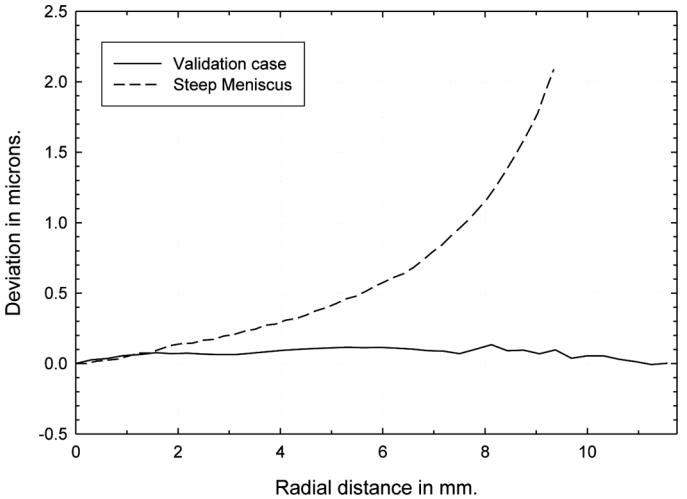

Figure 15 Sensitivity of the preform and mold shapes on deviation when the coefficient of thermal expansion is artificially set to zero. This analysis was done to isolate the effect of residual stresses. The 2-micron deviation for the steep meniscus lens arises when the gap was created and stays approximately constant until the end of the molding process.

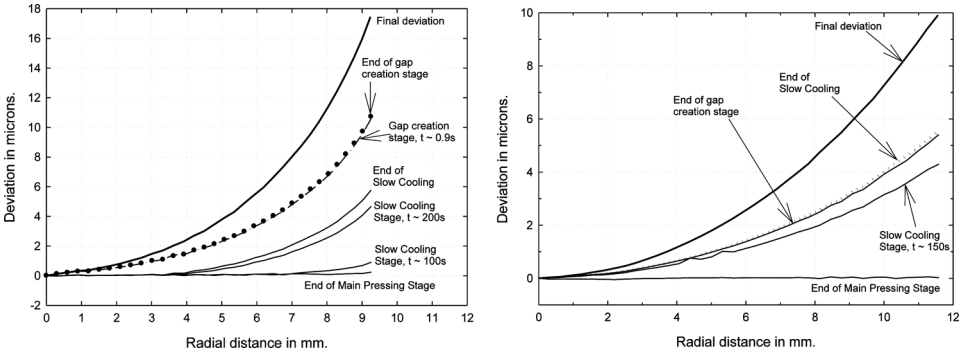

Figure 16 Time history of deviation for the steep meniscus lens in the upper portion of the figure and for the bi-convex lens in the lower portion.

the steep meniscus lens is basically in a state of axi-symmetric bending, while the stress state in the bi-convex lens is similar to that of tempered glass.

The "F_1" and "F_2" forces in Figure 17 that "pinch" the perimeter of the lens are also important, and therefore, the geometry of the periphery of the molds where the contact occurs during slow cooling is important. A slight change in geometry of the mold can shift the point of application of "F_1" and/or "F_2," which will alter the stresses in the lens, leading to a change in deviation. Because of this,when compensating the molds to achieve a desired lens shape to within one micron of accuracy, the geometry of the "edges" of the molds must be correctly treated, not just the aperture portion of the lens. A sensitivity analysis of this effect is considered in Part II.

It is important to emphasize that the results presented in Figures 16–18 are for the process conditions presented in Figure 8 and the material behavior presented in

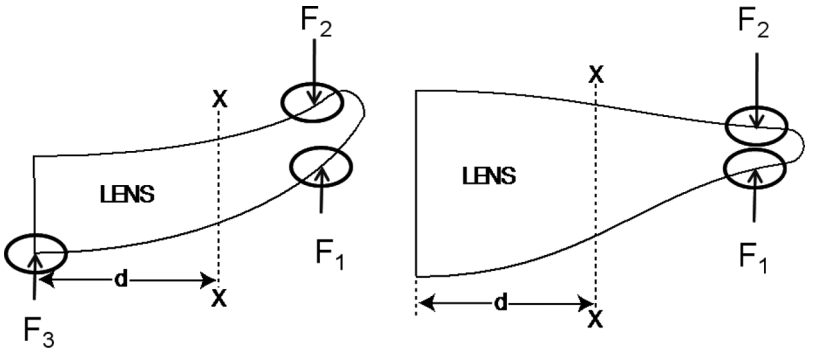

Figure 17 Schematic of the two lens geometries during the slow cooling stage when a maintenance force of 500N is applied to the lens. During this period the only regions of contact between the lens and the molds are indicated by circles. The net effect of this contact is to apply the forces indicated. When the maintenance force is removed, the force F_3 drops to zero and the meniscus lens on the left responds with an immediate shape change as shown in Figure 16. The dashed lines at a distance of $d = 5$ mm correspond to sections were the radial stress is plotted in Figure 18.

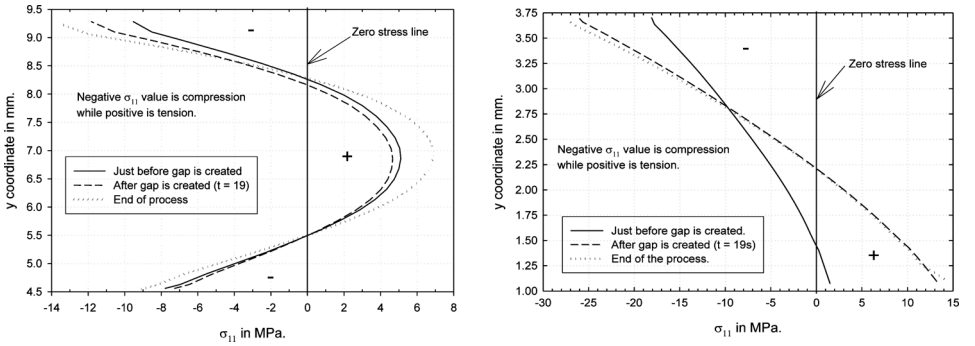

Figure 18 Radial stress states at the sections indicated in Figure 17 in the bi-convex lens (upper portion of figure) and steep meniscus (lower portion), at times corresponding to just before the gap is created, 19 seconds after the gap is created and at the end of the process, which corresponds to a residual stress state.

Tables 1–3, using Material Set 1. In particular, the maintenance force of 500 N was applied for 320 seconds before the gap opens. If this period were shorter, the stresses would have less time to relax, which would result in increased deviation due to this elastic response mechanism. Similarly, if a lower molding temperature was used for the same slow cooling period, the tendency of the deviation to increase due to this mechanism could increase since stresses decay more slowly at lower temperature. The key point is that the response of a lens to the opening of the gap could be very difficult to simulate accurately if there are large levels of stress present. As such, it could be difficult to compensate the molds for process conditions that lead to such stresses. For the case of a steep meniscus type lens, the deviation can be very dramatic if the gap is opened too soon, as the simulation indicates that the lens tends to curl upward.

CONCLUSIONS

A mathematical model was developed to simulate the precision lens molding process, taking into account process details and the complex material behavior of glass to predict the final profile deviation of the lens with micron level accuracy. The important processing stages included in the model are heating, soaking, pressing, gap creation and cooling. The developed computational model was defined and checked for convergence, a material property definition was presented and the deviations for a bi-convex lens and a steep meniscus lens were studied. The primary conclusion realized from the study showed that lens shape plays a significant role in how the final deviation is obtained, and that a complex part of the process for some lens shapes is the removal of the pressing force that creates a small gap. This study justifies and motivates a sensitivity analysis that includes both lens types. Furthermore, because of the complex evolving stress state and the manner in which shape change is achieved right after the gap opens, a very precise temperature-dependent characterization of stress relaxation is required, especially for the steep meniscus type geometry. Therefore, a significant experimental effort is required to characterize a glass type in order to rely on computational mechanics to make

reliable predictions. Most notably, structural relaxation and temperature dependent stress relaxation must be known with a high level of accuracy.

REFERENCES

1. M. Katsuki, Transferability of Glass Lens Molding, 2nd Intl. Symp. On Adv. Optical Manufacturing Technologies, edited by L. Yang, S. Wen, Y. Chen, E.-B. Kley, *Proc. SPIE Int. Soc. Opt. Eng.*, vol. 6149, pp. M1–M9, 2006.
2. R. O. Maschmeyer, C. A. Andrysick, T. W. Geyer, H. E. Meissner, C. J. Parker, and L. M. Sanford, Precision Molded-Glass Optics, *Appl. Opt.*, vol. 22, pp. 2410–2412, 1983.
3. A. Jain and A. Y. Yi, Numerical Modeling of Viscoelastic Stress Relaxation During Glass Lens Molding Process, *J. Am. Ceram. Soc.*, vol. 88, pp. 530–535, 2005.
4. G. C. Firestone, A. Jain, and A. Y. Yi, Precision Laboratory Apparatus for High Temperature Compression Molding of Glass Lenses, *Rev. Sci. Instrum.*, vol. 76, pp. 1–8, 2005.
5. A. Y. Yi and A. Jain, Compression Molding of Aspherical Glass Lenses-A combined Experimental and Numerical Analysis, *J. Am. Ceram. Soc.*, vol. 88, pp. 579–586, 2005.
6. A. Jain, G. C. Firestone, and A. Y. Yi, Viscosity Measurement by Cylindrical Compression for Numerical Modeling of Precision Lens Molding Process, *J. Am. Ceram. Soc.*, vol. 88, pp. 2409–2414, 2005.
7. S. M. Rekhson, Viscoelasticity of Glass, *Glass: Science and Technology*, edited by D. R. Uhlmann and N. J. Kreidl, vol. 3, pp. 1–118, 1986.
8. M. Brown, A Review of Research in Numerical Simulation for the Glass-Pressing Process, *Proc. I MECH E Part B, J. Eng. Manuf.*, vol. 221, no. 9, pp. 1377–1386, 2007.
9. A. Jain and A. Y. Yi, Finite Element Modeling of Structural Relaxation During Annealing of a Precision-Molded Glass Lens, *ASME J. Manuf. Sci. Eng.*, vol. 128, pp. 683–690, 2006.
10. A. Jain and A. Y. Yi, Finite Element Modeling of Stress Relaxation in Glass Lens Moulding Using Measured, Temperature-Dependent Elastic Modulus and Viscosity Data of Glass, *Modelling Simul. Mater. Sci. Eng.*, vol. 14, pp. 465–477, 2006.
11. H. Loch and D. Krause, *Mathematical Simulation in Glass Technology*, Springer, New York, 2002.
12. G. Scherer, *Relaxation in Glass and Composites*, John Wiley and Sons, New York, 1986.
13. S. H. Chang, Y. M. Lee, T. S. Jung, J. J. Kang, S. K. Hong, G. H. Shin, and Y. M. Heo, Simulation of an Aspheric Glass Lens Forming Behavior in Progressive GMP Process, *NUMIFORM '07, Mater. Process. Design*, pp. 1055–1060, 2007.
14. J. W. Na, S. H. Rhim, and S. I. Oh, Prediction of Birefringence Distribution for Optical Glass Lens, *J. Mater. Process. Technol.*, vols. 187–188, pp. 407–411, 2006.
15. M. Sellier, C. Breitbach, H. Loch, and N. Siedow, An Iterative Algorithm for Optimal Mould Design in High-Precision Compression Molding, *Proc. I MECH E Part B J. Eng. Manuf.*, vol. 221, no. 7, pp. 25–33, 2007.
16. C. V. Madhusudana *Thermal Contact Conductance*, Springer, New York, 1995.
17. M. Arai, Y. Kato, and T. Kodera, Characterization of the Thermo-Viscoelastic Property of Glass and Numerical Simulation of the Press Molding of Glass Lens, *J. Therm. Stresses*, vol. 32, pp. 1235–1255, 2009.
18. J. H. Li and D. R. Uhlmann, The Flow of Glass at High Stress Levels: I. Non-Newtonian Behavior of Homogeneous 0.08 $Rb_2O{\cdot}0.92$ SiO_2 Glasses, *J. Non-Crystall. Solids*, vol. 3, pp. 127–147, 1970.
19. A. Q. Tool, Relation Between Inelastic Deformability and Thermal Expansion of Glass in its Annealing Range, *J. Am. Ceram. Soc.*, vol. 29, pp. 240–253, 1946.

20. O. S. Narayanaswamy, A Model of Structural Relaxation in Glass, *J. Am. Ceram. Soc.*, vol. 54, pp. 491–498, 1971.
21. C. T. Moynihan, A. J. Easteal, M. A. Debolt, and J. Tucker, Dependence of the Fictive Temperature of Glass on Cooling Rate, *J. Am. Ceram. Soc.*, vol. 59, pp. 12–16, 1975.
22. S. Gaylord, Thermal and Structural Properties of Moldable Glass Types, Master's thesis, Clemson University, Clemson, SC, December 2008.
23. Specification Sheet for L-BAL35 glass, Ohara, Japan. (www.ohara-inc.co.jp).
24. Specification Sheet for Tungsten Carbide Material, Kennametal Inc., Latrobe, PA, USA. Available at: www.Kennametal.com
25. L. Duffrene, R. Gy, H. Burlet, and R.Piques, Multiaxial Linear Viscoelastic Behavior of a Soda-Lime-Silica Glass Based on a Generalized Maxwell Model, *J. Rheol.*, vol. 41, pp. 890–895, 1997.
26. B. Ananthasayanam, *Computational Modeling of Precision Molding of Aspheric Glass Optics*, Ph.D. Dissertation, Clemson University, Clemson, SC, December 2008.
27. A. Markovsky, T. F. Soules, V. Chen, and M. R. Vukcevich, Mathematical and Computational Aspects of a General Viscoelastic Theory, *J. Rheol.*, vol. 31, pp. 785–813, 1987.
28. S. Gaylord, B. Ananthasayanam, L. Petit, C. Cox, U. Fotheringham, P. F. Joseph, and K. Richardson, Thermal & Structural Property Characterization of Commercially Moldable Glasses, *J. Am. Ceram. Soc.*, vol. 93, pp. 2207–2214, 2010.
29. G. Scherer and S. M. Rekhson, Viscoelastic-Elastic Composites: II, Sandwich Seal, *J. Am. Ceram. Soc.*, vol. 65, pp. 399–406, 1982.